SHiP Technical Proposal:

Questions from the SPSC Referees

September 23, 2015

In this document we have collected all questions posed by the SPSC Referees in their 25/5/2015 mail and our corresponding replies. Some of them have been answered in the Addendum to the Technical Proposal and are not repeated here.

A) General

1. *A critical aspect will be to convince the Council that CERN is the best place for such a facility, considering that FNAL and JPARC are already devoted to the high intensity frontier. In section 2.2 and Appendix B, some arguments are given involving e.g. charm production cross sections, length of muon shield, length of decay region, detector acceptance and cost, etc to conclude that the 400 GeV SPS energy is optimal. However the discussion remains quite qualitative. Would it be possible, using a toy model parameterizing the dependence on the main inputs, to provide more quantitative plots showing where the optimal point for a given efficiency at a given cost is? For example, how does the background rate scale with the cavern size? This would also be useful to further fine tune the overall setup (energy, etc...) to optimize the cost.*

   Answer provided in the Addendum.

2. *To what extent are the detector layout choices simultaneously optimal for the various searches being carried out? For each of the main signals being searched for how different would an optimal detector look compared to the current design?*

   The detector has been designed to be sensitive to all final states listed in Table 2.1 of the TP [3], regardless any assumption on the nature of the mother particle. However the geometrical acceptance of the detector depends on the production mechanism of the mother particle and on its lifetime, hence it is model-dependent. While fixing the transverse dimensions of the spectrometer to its maximal affordable size in terms of cost, we studied the variation of the acceptance as a function of the vacuum vessel length for three portals, neutrino, dark photon and dark scalar. The results are shown in Fig. 1. We see that the dark scalar portal would prefer a vacuum vessel ~ 10 m shorter than the baseline due to the shorter lifetime and the larger $p_{\rm T}$ of the products of b decays. More detailed studied will be performed for the Technical Design Report.

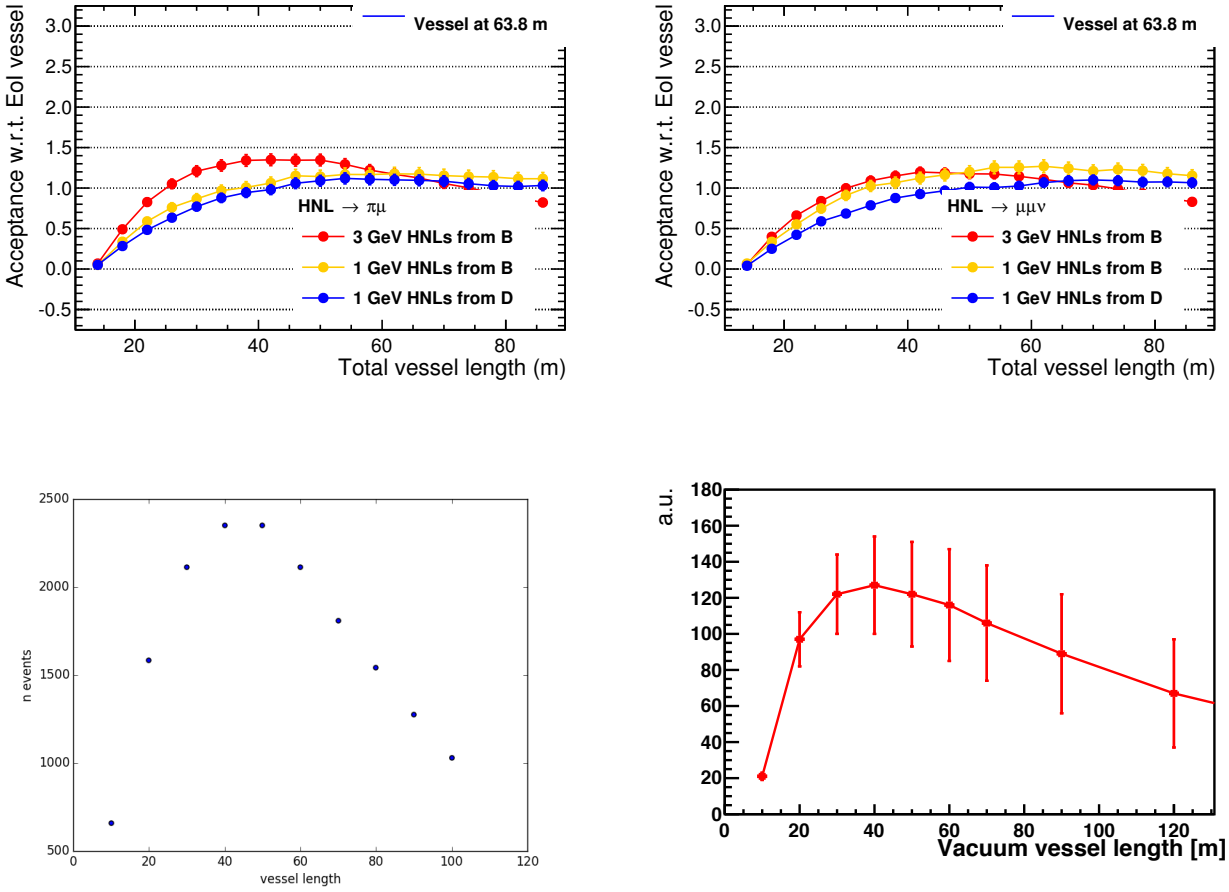

Figure 1: Acceptance for $HNL \to \pi^+\mu^-$ (top left) and for $HNL \to \mu^+\mu^-\nu$ (top right) produced via a charm decay with mass m = 1 GeV/c^2 (top left), for a dark photon produced via proton bremsstrahlung with coupling $\epsilon = 10^{-7}$ and mass 1 GeV/c^2 (bottom left) and for a dark scalar produced via a b decay with mass of 1 GeV/c^2 and coupling $y^2 = 10^{-9}$ (bottom right) as a function of the length of the decay volume for an elliptical vessel with transversal sizes of 5×10 m^2.

3. *By the time SHiP starts producing first results, to what extent can one expect todays limit on various SHiP signals to have evolved? E.g. it would be instructive to have versions of the main figures 5.19-5.38 with also projections of other experiments that are currently either running or approved, or being currently proposed.*

   Answer provided in the Addendum.

B) Schedule and Resources

1. *Final approval of the project is not expected before the TDR is released in 2018, but civil engineering for the beam transfer has to start right at the beginning of LS2. Can you quantify how much resources have to be committed before LS2 (design, tendering, ordering, etc...) to ensure a timely start of civil engineering at the beginning of LS2?*

   Answer provided in the Addendum.

2. *In table 6.2 what is the part of the facility cost (135.8MCHF) and specifically of the civil engineering cost (57.4 MCHF) devoted to what has to be done in LS2 ? What is the minimum delay between the effective commitment of this part and the actual start of the work?*

   Answer provided in the Addendum.

3. *If the LS2 work were performed instead in LS3, what would the impact be on the rest of the programme?*

   Answer provided in the Addendum.

C) Apparatus and Detector

1. *Muon shield / section 3.4: Quite some details are given on the muon active shield, whereas the passive shield is concluded not to be sufficient if alone. We however understand that some passive shielding will be provided to complement the active shielding. What is the expected layout?*

   It is not foreseen to add passive shielding to protect against muons. Any passive material in the way of the muons is more of a hindrance than a help. However, we are considering to add shielding to protect the Veto counters from EM-showers which accompany the deflected muon beam. The development of this shielding is work in progress.

2. *Muon spectrometer / section 4.3: You mention the possibility to recover the OPERA RPCs. What are the prospects to recover the OPERA magnets as well?*

   We plan to recover the OPERA magnets as well.

3. *The straw detectors are essentially an evolution to larger dimensions of the NA62 straws. How do you control the sag of the wires and the straws (absolute and with respect to each other)?*

   We are currently investigating the effect of the wire offset on the $t(r)$ relation (drift time versus position) with GARFIELD simulations, see Sec 4.7.2.1 of TP [3], and we plan to complement this study with detailed measurements in controlled experiments in the

laboratory and with a test-beam setup. The 50 straws from Dubna (∼5 m long) will be assembled in a prototype straw module and used to measure the wire sagging and straw deformation. Measurements of the signal attenuation will also be performed. A smaller straw prototype has been produced and will be used to measure the $t(r)$ relation as a function of varying (measured) wire offset. For this, an optical system for measuring the straw edge and wire position by transparency will be developed. A track telescope will be used to define the track position in the straw under study. Based on our findings we will define how much sagging of the straws and wires can be tolerated and develop a mechanical support accordingly (which may well be inspired by the NA62 design).

4. *Are precautions needed when changing the pressure in the decay vessel to limit bending of the straw tubes by the airflow? (This is a consideration in NA62). How long do you think it takes (also in this context) to pump down to* 10^{-3} *mbar?*

   Indeed, the change of pressure and air flow in the vacuum vessel during pump-down or venting is a consideration in both NA62 and SHiP. A force on the straws can arise due to a pressure gradient across a straw plane which acts as a flow resistance. This effect takes place only in rough vacuum ($1 - 1000$ mbar) and can be reduced by judicial use of flow restrictions at the pumping ports and of bypass conductances over the straw planes, while maintaining an acceptable pump-down time (a few hours). It was successfully achieved in NA62. Our setup, in that respect, is quite similar and will differ mainly by the vessel volume and the straw length. A detailed assessment will be performed and included in the Technical Design Report.

5. *For the straw tubes and drift tubes is there any gain loss from space charge due to the 50 kHz of muons passing through? Is this included in the estimated tracking performance in section 4.7.2?*

   We assume that the *50 kHz of muons passing through* comes from p. 125, section 4.11 "Muon detector", where we state: *Preliminary simulation studies (see Section 5.2.1.3) show that the flux of muons is 50 kHz over the entire muon detector area of (6 × 12)* m^2*, corresponding to a rate of < 0.1 Hz/cm*^{2}. Concerning the Hidden Sector straw tracker, as stated on p.93 of the Technical Proposal, background simulation studies indicate that we could expect a total hit rate per tracking station of the order of 10^7 hits per spill of 1 s. The maximum rate on a single straw is about 2 kHz. At this rate we expect negligible space charge effects.

6. *How do you plan to align the different detector elements?*

   Simulation shows that we will have several kHz of muons with $p > 3$ GeV/c which eluded the muon-shield and that can be reconstructed by the spectrometer. These will be used to time and position align the different elements of both the tau neutrino detector and the Hidden Sector detector. If the muon shield works "too well" we could always reduce the B-field in especially the first magnet to increase the number of large momenta muons which elude the shield.

7. *What is the effect of the B field non-uniformity in the various magnets on the tracking performance? Particularly where magnets will be re-used, eg GOLIATH, do non-uniformity*

measurements exist and can these be used to estimate the systematics associated with the field non-uniformity on, e.g., DOCA cuts, vertex cuts, target impact parameter cuts. Is the precision of the field maps good enough and will the magnet fields be mapped again once in place with all the other equipment (eg. the Muon magnetic spectrometer)?

SHiP intends to map the field in both magnets using a CERN built measurements bench, which allows moving Siemens KSY44 Hall probes through the entire magnetic volume, with all the surrounding magnetic elements in place. Each sensor holds three probes, one for each component of the magnetic field, B_x, B_y and B_z.

With this system a precision of a mTesla and a fraction of a mm has been achieved, allowing LHCb to measure $dp/p \sim 0.5\%$ over their whole momentum range. Goliath will be used to determine the charge of particles, corresponding to $dp/p \sim 20\%$, hence the above mapping is a huge overkill, and with coarse steps could be done in one day. The Hidden Sector spectrometer aims at $dp/p \sim 0.5 - 1\%$ in which its main contribution is due to the multiple scattering component. Hence, again the field precision will not contribute. The DOCA, vertex and impact parameter resolutions are dominated by multiple scattering in the straw chambers, and the distance of the vertex from its first chamber.

8. *The density of muon tracks is about 1 per (20 μm)^2 in the emulsion after 6 months' exposure (for 4 kHz/m^2); the real-time tracking has a resolution of about 100 μm. So that means 25 emulsion tracks per target tracker resolution window. Have simulations been performed to explicitly establish the ease of extraction of signals among all of these tracks? How much does the target tracker really contribute in correctly linking tracks across bricks.* We have estimated an integrated muon flux in 6 months exposure of about 1000/mm^2. It is indeed one in (30 μm)^2 as pointed out by the referees, equivalent to about 10 tracks in the target tracker window of (100 μm)^2 in 6 months. It is worth noting that this flux is integrated over the whole angular spectrum. Tracking in the emulsions with such a track density was proven to be successful by the DONUT and E653 experiments. Penetrating tracks will be easily identified and discarded in the brick. The remaining stopping tracks will be used to identify neutrino interaction vertices. Tracks originated from neutrino interactions are projected on the target tracker plane (TT) immediately downstream. In the TT window we expect 10 hits integrated in 6 months plus the one from the neutrino interaction. The hits originated from penetrating muons will be discarded by the time coincidence with hits in the upstream TT planes. The remaining hit will be associated to the neutrino event. All the hits with the same time stamp will be used to track the muon (from tau decay or muon neutrino interaction) across the target and to connect it to the muon spectrometer downstream.

9. *Tau neutrino selection / sections 4.2.1.5 and 5.4: Highly selective procedures will be necessary to isolate the $O(10^3)$ tau neutrino events from the $O(10^5)$ neutrino interactions. You mention automatic scanning procedures to identify the neutrino interactions, and kinematic cuts to identify the tau neutrino ones. Our understanding from the OPERA procedures is that there is still need for significant visual scanning in the final analysis steps, though the final sample is only 4 tau candidates and O(100) charm events. Can you extrapolate from the OPERA experience what will be the load for visual scanning in the SHIP analysis ?*

The visual inspection in OPERA is motivated by two problems: tracing inefficiency and impurity caused by Compton electrons. The first problem is due to the original refreshing treatment and to the emulsion aging: OPERA films are indeed now almost 15 years old. We have experienced the extremely good performance of fresh emulsion films and a progressing deterioration of their quality with time. The second problem is due to the long-term contact of emulsion films with lead. Compton electrons are indeed produced by the lead radioactivity. Both problems will not occur in SHiP because the emulsions will be produced shortly before the exposure. Moreover the exposure will last only 6 months, thus making fading and radioactivity effects negligible. In these conditions fully automated reconstruction is certainly viable.

10. *Software/ section 4.13: you mention the adoption of FAIRROOT as the general software framework of SHiP. We understand the advantage of using an available environment. However FAIRROOT seems to be presently used onnly by future experiments, an dnot really validated in a realistic operational environment. Since you already use it for your performance evaluations, can you give indications to which level it is already validated and debugged?*

    FairRoot is a framework integrating the Geant3 and Geant4 Monte Carlo transports engines and a large number of particle generators (Pythia, Pluto, etc) in an environment making heavy use of the ROOT system services for data storage, geometry, analysis, graphics, etc. The individual components have all been extensively validated by many experiments, notably all the LHC experiments.

    The combination of these components in the FairRoot framework has been in use by the FAIR experiments for test beam studies since 2011. In addition FairRoot is being used by the R3B experiment[1], the ASY-EOS experiment[2] and, last but not least, FairRoot is at the heart of the new ALICE O2 combined online/offline framework.

    By using FairRoot SHiP has chosen a framework which has a well defined and guaranteed support model and a thriving developer community, guaranteeing that SHiP computing will be able to make efficient use of modern computing hardware for the foreseeable future.

11. *Does the neutrino detector in any way diminish the sensitivity of the HS detector? If it does, have you considered moving it behind the main detector (though this would of course reduce the neutrino flux by $\sim \times 4$)?*

    Figure 2 shows the layout of the active muon shield as shown in Figure 3.10 of the SHiP Technical Proposal [3], but in addition the outline of the ν_τ detector elements and the start of the vacuum vessel has been indicated.

    The shield has been designed to fulfill the following boundary conditions:

    - The largest momenta muons, i.e. muons up to 350 GeV/c, should be bend outside the acceptance of the hidden particle decay volume of the vacuum vessel.

[1] http://iopscience.iop.org/1742-6596/523/1/012034.
[2] http://pro.ganil-spiral2.eu/events/workshops/iwm/2011/presentations/russotto-iwm2011.

- The internal radius of the decay volume is 2.5 m, which with the wall thickness and the 30 cm of liquid scintillator gives an outside radius of 2.85 m. The radius is the same for the complete vessel to allow easier construction.
- The decay vessel is preceded by a 5 m long V^0-decay-vessel, followed by the straw-veto-tagger. The radius of this vessel can be adapted to the muon flux radius.
- Provide 10 m of space between the shield and the V^0-decay-vessel for the ν_τ detector elements. The radii of these elements will be adapted to the muon flux.

As is shown in Figure 2 the largest momentum muons just miss the outside radius of the decay vessel which starts 63 m after the hadron stopper. In addition, the shield is constructed so that low momentum muons also just miss the decay vessel. The other detector elements fit in the region $48 < z < 63$ m, 10 m for the ν_τ detector, and 5 m for the V^0-decay-vessel. The radii of these elements have been adapted to avoid the local muon flux. It should be noted that the existing Goliath magnet happens to have exactly the allowed width.

Now suppose we would have dropped the last condition, i.e. do not foresee 10 m of space for the ν_τ detector, and try to move the hidden particle decay volume as close as possible to the hadron stopper. This requires that the largest momentum muons pass through more field, i.e. the active shield has to be extended. Figure 3 shows the layout of such an active muon shield. The shield has been extended by an extra 7 m to bend the 350 GeV muon out to a radius of 2.85 m, 5 m downstream of its end. The shield cost increases by an estimated 15-20 %. This allows the hidden particle decay volume to start at 60 m, leaving the required 5 m for the V^0-decay-vessel.

Hence, the hidden particle spectrometer moves from a distance of roughly 120 m to 117 m from the target. The emulsion of the ν_τ detector moves from 57 m distance from the target to roughly 130 m. The negligible gain in acceptance for hidden particles should be compared to a factor 3.5 to 7 loss in acceptance depending on the neutrino flavour. In addition, the muon spectrometer of the ν_τ detector acts as active last material before the hidden particle spectrometer by tagging any ν interaction, and this feature to tag a background source would be lost, with a corresponding background increase.

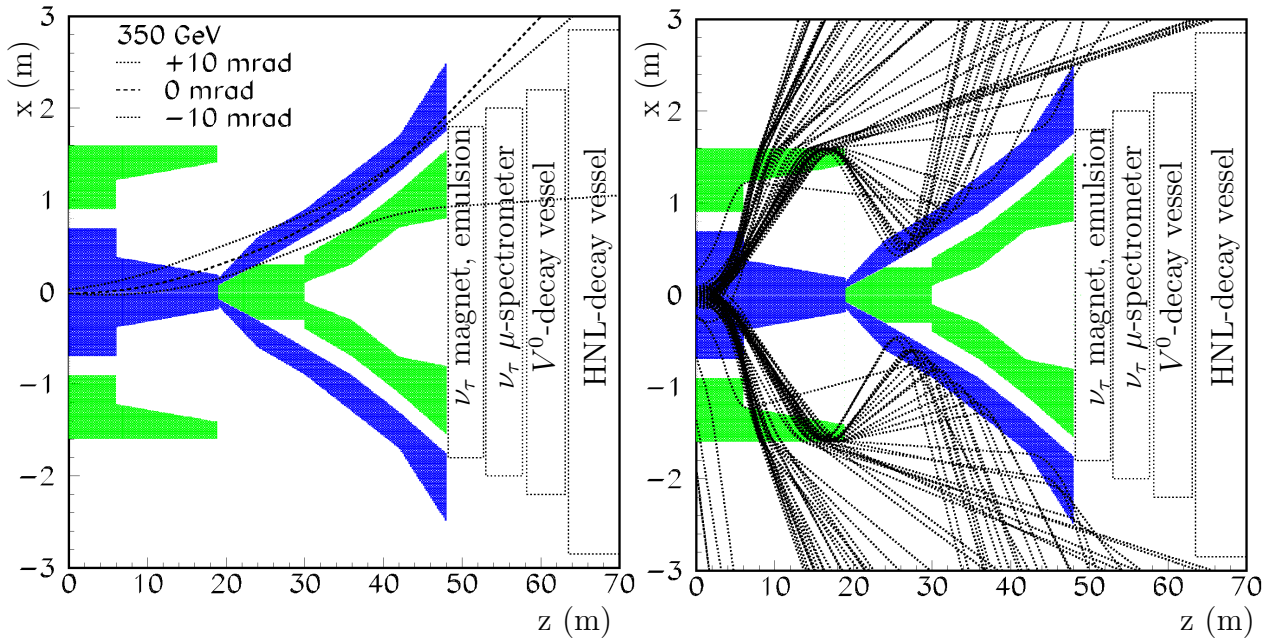

Figure 2: The x, z configuration of a possible active muon shield. The blue and green show the regions of field and return field respectively. Also sketched are the outlines of the various detector elements. On the left the trajectory of three 350 GeV muons with a range of initial angles. On the right the shield is overlayed with a selection of low momentum muon trajectories.

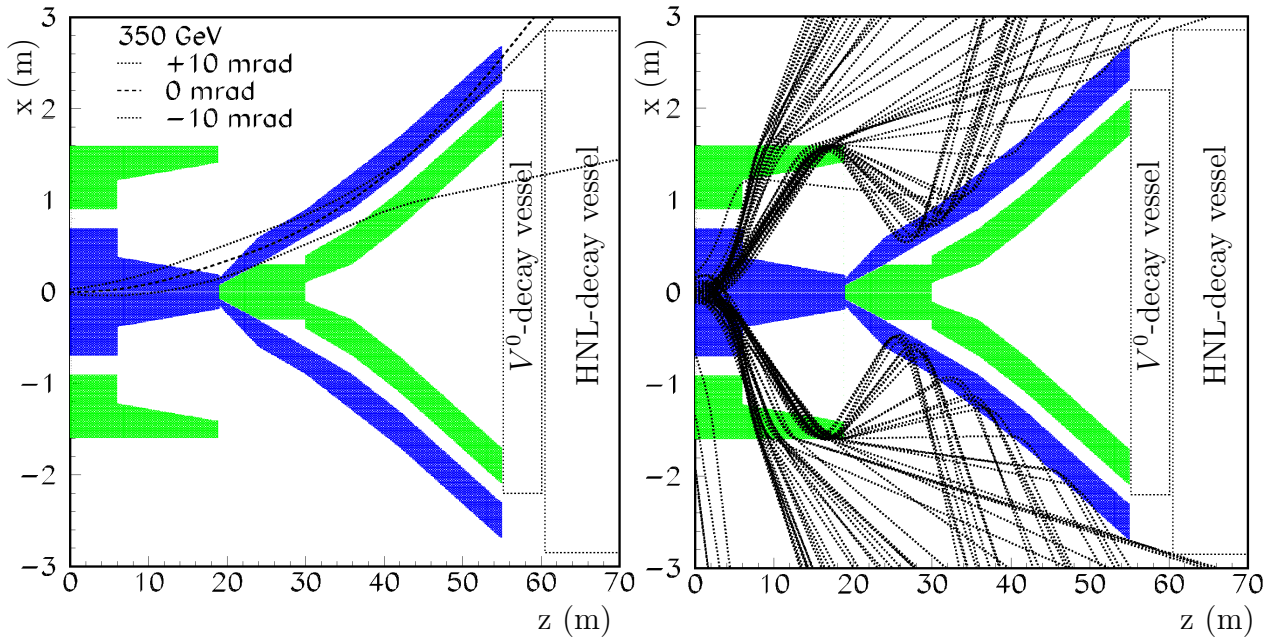

Figure 3: The x, z configuration of an active muon shield without a provision for the ν_τ detector. The blue and green show the regions of field and return field respectively. On the left the trajectory of three 350 GeV muons with a range of initial angles. On the right the shield is overlayed with a selection of low momentum muon trajectories.

D) Background

1. *There will be large numbers of muons to be deflected. Can a non-vanishing number of them be scattered back into the region of interest by the material in the active-shield area?*

   This answer also addresses part of question A1, i.e. how does the muon rate scale with the caven size. All the material in the active shield area including the cavern walls are in the simulation, and back scattering is simulated. In fact, a significant part of the low energy background originates from muons scattering in the walls of the small tunnel containing the first magnet (Fig. 4, left). A further optimization done after submission of the TP shows that this could be reduced by about a factor 10 by making the first part of the cavern as wide as the rest (Fig. 4, right). Work in progress, see also answer to D.2

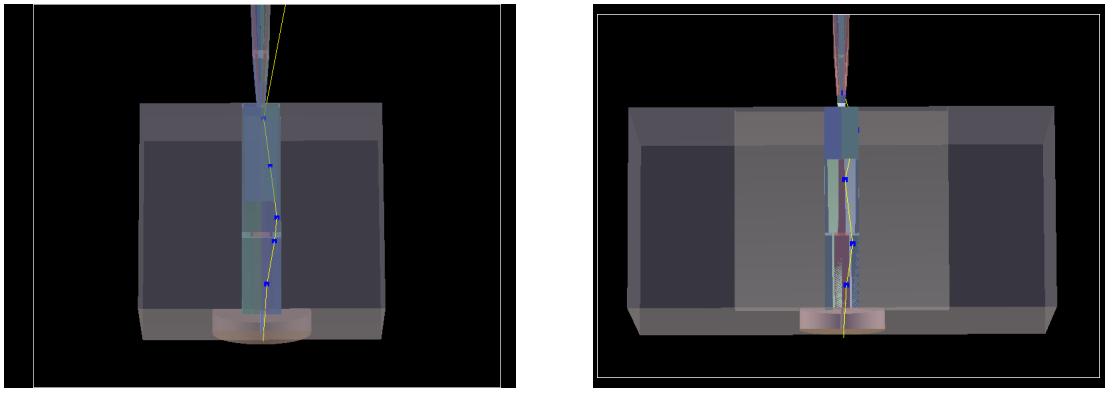

Figure 4: Sketch of muons back-scattered from the walls of the tunnel containing the first magnet of the active muon shield: with lateral dimensions of 3.5 m as in the TP (left) and of 20 m (right).

2. *We have some difficulty reconciling the different numbers for muon rates at different parts of the detector (e.g. 4 kHz/m^2 at neutrino detector, 100 kHz at upstream veto tagger and 7 kHz in the spectrometer). It would be useful to have $x - y$ plots of the muon flux at the various positions of these detectors, and the incident rates summarized in a table like 4.12.*

   Here we have to distinguish between hit rates, like 100 kHz at upstream veto tagger, and reconstructed track rates, like 7 kHz in the spectrometer. Different hit rates for different detector positions are shown in the following figures: Figure 5 shows the overall hit rate for various detectors, Fig. 6 shows the hit rates induced only by muons, Fig. 7 shows the hit rates induced by muons with $p > 3$ GeV/c. The numbers in each plot correspond to the integrated rate of hits / spill for $N_{\rm pot} = 5 \times 10^{13}$/spill. It is worth noticing that a large fraction of the hit rate induced by muons originates from muons back-scattered by concrete walls in the small tunnel containing the first magnet of the active muon shield. Figures 6 and 8 show the hit rates induced by muons assuming a lateral dimension of the tunnel of 3.5 m (as in the TP) and 20 m (as the rest of the cavern), respectively: the hit rate decreases by a factor of ten. Detailed studies will be performed for the Technical Design Report.

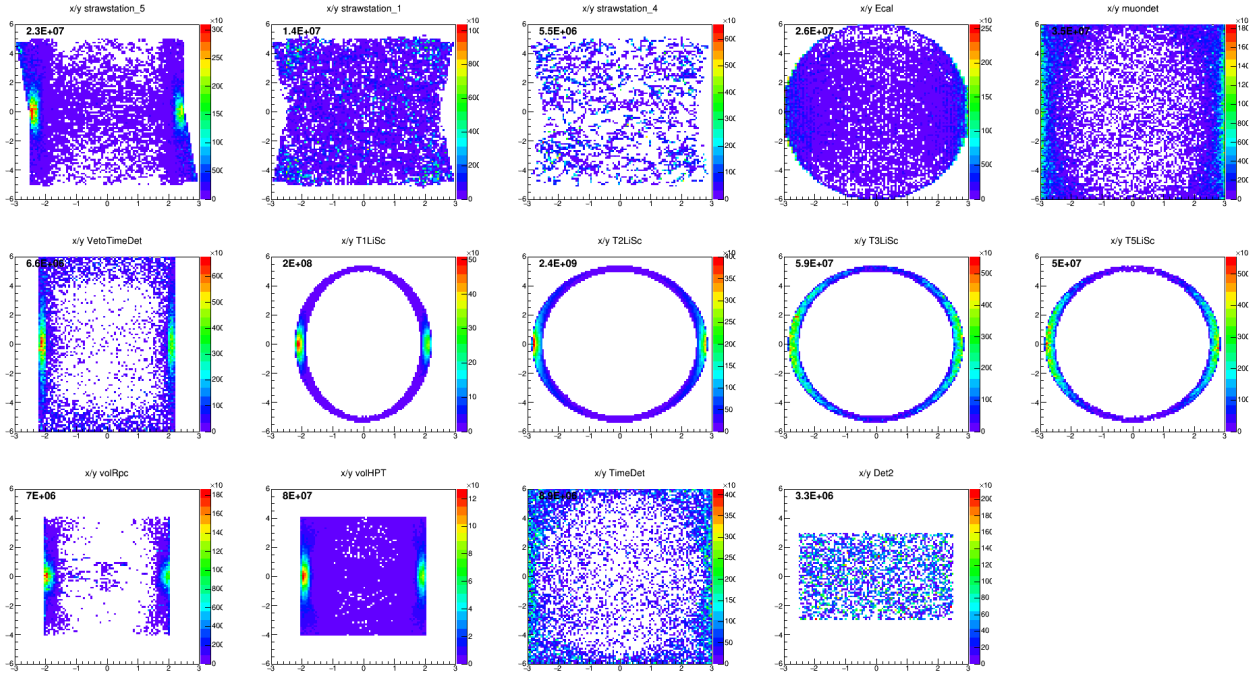

Figure 5: Overall hit rates seen by various detectors during 1 sec spill of 5×10^{13} pot.

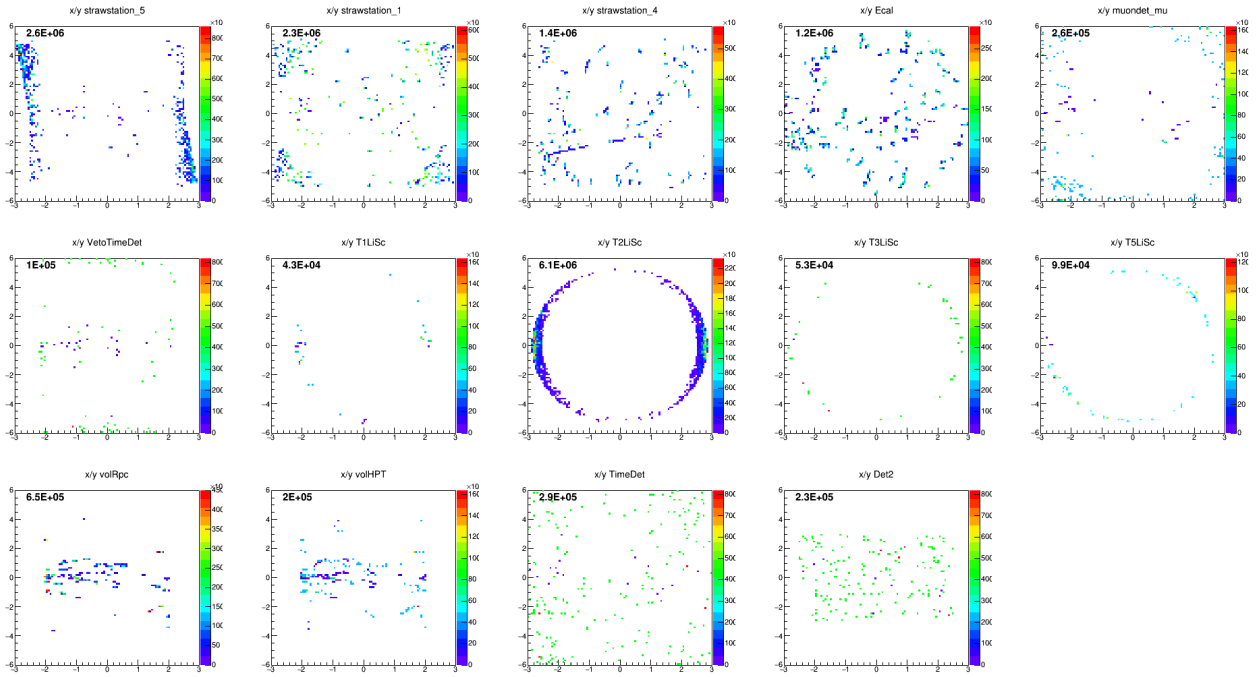

Figure 6: Hit rates induced by muons seen by various detectors during 1 sec spill of 5×10^{13} pot.

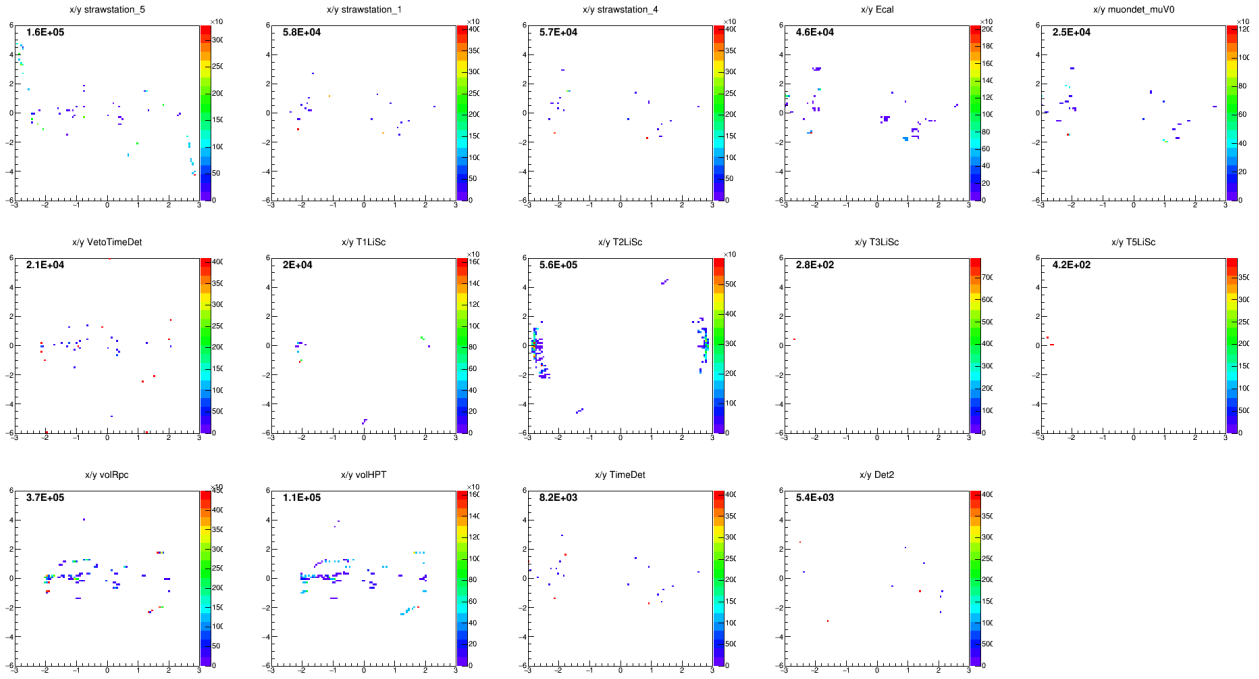

Figure 7: Hit rates induced by muons with $p > 3$ GeV/c seen by various detectors during 1 sec spill of 5×10^{13} pot.

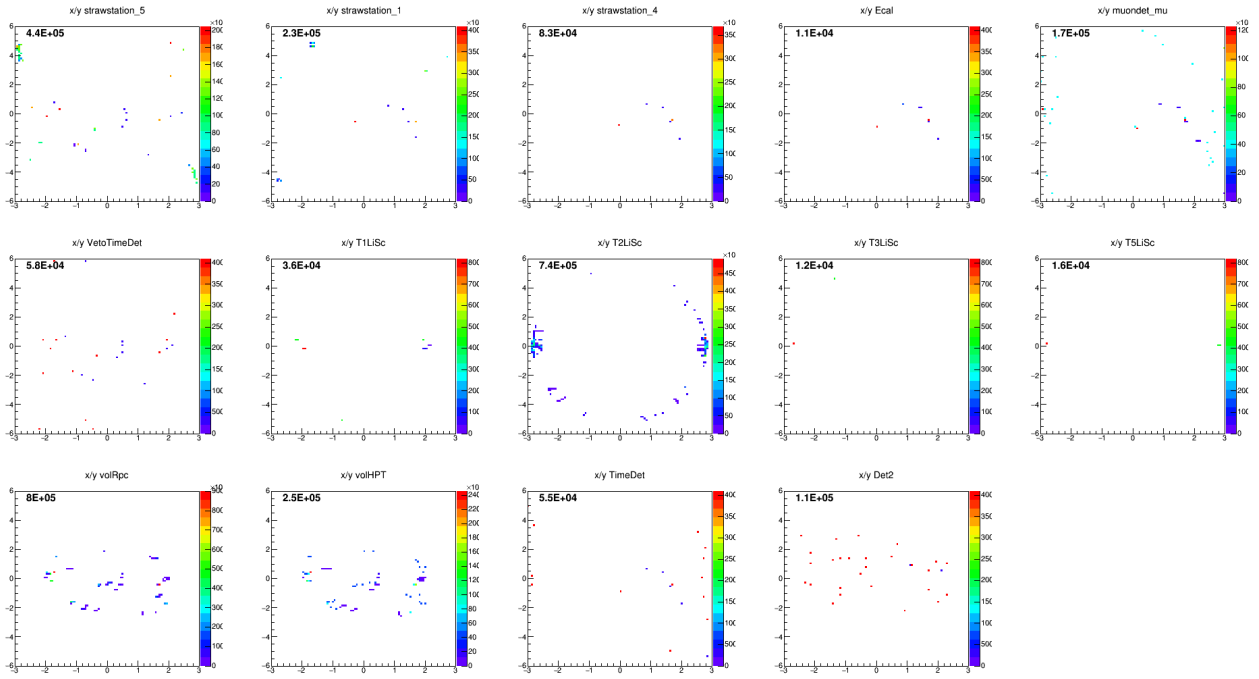

Figure 8: Hit rates induced by muons seen by various detectors during 1 sec spill of 5×10^{13} pot after having increased the tunnel containing the first magnet of the active muon shield from 3.5 m to 20 m

.

3. *Similar plots would be useful for the neutrino flux.*

   Figure 9 shows a neutrino tomography of the experimental setup and Fig. 10 the xz and yz projections. The points define the position of the potential interaction with the experimental setup of neutrinos originating from the target, the density of points reflects the material density.

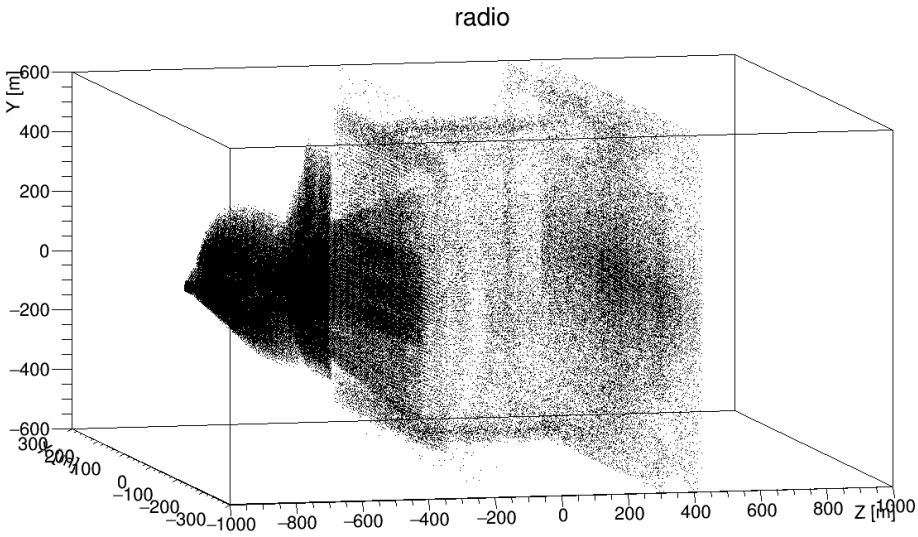

Figure 9: Neutrino tomography of the experimental setup. The points define the position of the potential interaction with the experimental setup of neutrinos originating from the target, the density of points reflects the material density.

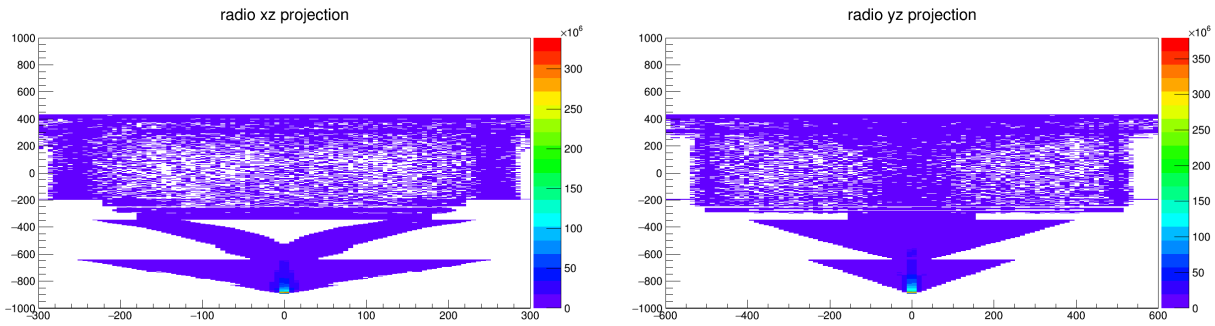

Figure 10: Neutrino tomography of the experimental setup: xz view (left) and yz view (right). The points define the position of the potential interaction with the experimental setup of neutrinos originating from the target, the density of points reflects the material density.

4. *Have you estimated the overall background rates from a combination of a neutrino background with a muon being present in a narrow time window, i.e. pileup of the muon background on top of the neutrino background?*

   For 7 kHz rate of muons the probability to have a muon in a 340 ps window is 2.4×10^{-6}. For $\sim 10^7$ neutrino interactions in 5 years ($5 \cdot 10^6$ sec) the probability to have a neutrino interaction in 340 ps is 6×10^{-10}. Hence the probability to have a neutrino-muon combinatorial background is much smaller than the di-muon one.

5. *Figure 4.42 shows a large amount of material, e.g. services, placed a couple of meters on either side of the decay vessel. What is the background that comes from muon scattering on this material?*

   This is a conceptual view, the various auxiliary services are placed in a way that they are visible for demonstration. The distribution of material in the cavern needs to take into account the muon flux, which is mainly in the horizontal plane. So, this material will be distributed to top and bottom of the detector. When we have more detailed technical drawings, we will put this material in the simulation to verify that does not induce further background.

6. *Table 5.4 and subsequents:*

   (a) *e.g. last row of 5.4: 1.5% of 14.7 would give 0.2 events; scale by 2 for muon bkgd and you get 0.4; so it would be good to have the statistical uncertainties on the numbers being quoted.*

   Answer provided in the Addendum.

   (b) *It would be useful to have a table for the golden mode, $HNL \to \pi\mu$, with the set of cuts, the signal rate after each cut, and the background rates after each, separated according to the individual backgrounds, e.g. neutrino, combinatorial muons and muon scattering products. (Currently in section 5.2.1, each background gets discussed with different cuts, e.g the DOCA cut of <30 cm for the neutrino background, 3 cm for the muon inelastic scattering background, 1 cm for the muon combinatoric background).*

   Answer provided in the Addendum.

   (c) *We had difficulty reproducing the numbers in section 5.2.1.3: both the 10^{-7} from the timing requirement and the overall 0.1. It would also be useful to add a column to table 5.5 showing the efficiency of the individual cuts, to help understand their individual impact.*

   Answer provided in the Addendum.

E) Sensitivities

1. *Considering figs. 5.19-5.23, how do the sensitivities depend on the number of p.o.t. E.g. suppose that* $2 \cdot 10^{20}$ *pot is challenging and only* 10^{20} *gets delivered, how will the sensitivity plots change?*

   Answer provided in the Addendum.

F) Systematics

1. *Systematics on signal: for accurately setting the limits, and especially for some of the measurements planned in the neutrino programme, its important to have good knowledge of the fluxes and angular distribution both of heavy-mesons and of the neutrinos. What are the current expected systematic uncertainties, how do they affect the quality of the final results and to what extent is there for scope for improvement?*

   Indeed, the choice of the fragmentation variable for the $c \to D$ transition, which at high $p_{\rm T}$ is irrelevant, may lead to some differences at small $p_{\rm T}$, where non-factorizable effects can be significant. The ensuing non-perturbative uncertainty is, however, expected to be not larger than the perturbative ones. For example in FONLL, that we have used, the shifts in the rate are at the level of 10%. One way to study the systematic would be to consider different choices of fragmentation. The exercise would consist in comparing differential rates obtained assuming $p(D) = z \cdot p(c)$, the three-momenta being taken in the laboratory frame (i.e. what was done so far) with alternative prescriptions as $p_{\rm T}(D) = z \cdot p_{\rm T}(c)$and $y_D = y_c$ or $(E+p)_D = z \cdot (E+p)_c$.

2. *Systematics on backgrounds: what are the major contributing sources expected to be, e.g. interaction cross sections, muon pile-up, timing and spatial alignment precision, non-uniformity of detector response, etc. Given reasonable estimates for the most important systematics, what is the impact on the signal sensitivity of the flagship measurement channels?*

   It is at the moment under investigation but we do not expect this to change our final conclusions.

3. *For the proton strangeness measurements: there are a number of potential systematic effects, such as nuclear corrections, higher twist effects, etc. How might these uncertainties affect the strangeness extraction? And is it possible to have a plot of the distribution of data over* (x, Q^2) *(e.g. kinematic plane with some colour-coding for statistics as a function of* x, Q^2*) to help judge the impact of cutting out the low-*Q^2 *region?*

   In order to reduce the impact of higher twist effects, the standard cuts applied in the NNPDF analyses have been imposed to the generated pseudo-data. These include a cut on Q^2 ($Q^2 > 3.0$ GeV^2) and the invariant mass of the final state ($W^2 > 12.5$ GeV^2).

In Ref. [5] it has been shown that the impact of nuclear corrections on PDF determinations based on the NNPDF methodology is negligible in comparison to the typical uncertainties of the scattering data of heavy, approximately isoscalar, targets.

For this reason no nuclear corrections have been applied to the data. In view of the higher precision expected for the data coming from the SHiP experiment, this conclusions should, in principle, be reassessed. In this preliminary study we have not performed any investigation of the impact of these theoretical uncertainties on the strangeness extraction. We defer this analysis to a future study where this question will be addressed by performing a number of fits applying different Q^2 and W^2 cuts and different models for nuclear corrections.

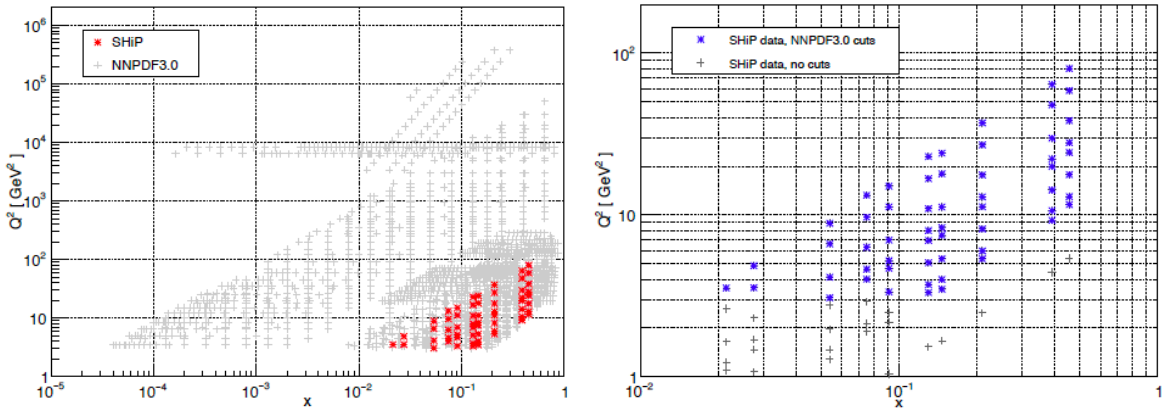

Figure 11: Left plot: SHiP data (red) are reported in the (x, Q^2) plane together with all the data used by the NNPDF group (grey). Right plot: SHiP data in the same plane with (blue) and without (grey) the selection applied.

4. *A related question: there is presumably an uncertainty on the p_T distribution of D mesons (and so the number of tau neutrinos that reach the detector): how much does this affect potential precision of the results, e.g. specifically for the extraction of the F_4 and F_5 structure functions?*

   The uncertainty in the p_T distribution has been accounted for by changing the renormalization and factorization scales in the computation. This translates into a $\pm 20\%$ error on the flux that was accounted for in the sensitivity for F_4 and F_5 structure functions.

G) Resources and costs

1. *Significant R&D and engineering is needed to finalise the beam (section 3.2.1), the target (section 3.3.3) and the muon shield (section 3.4.3). These activities are expected to extend at least up to the TDR in 2018, but table 6.1 lists only limited resources in 2015 and 2016 only. Can you better quantify the CERN resources needed up to 2018 to finalise the facility design at the level expected for the TDR?*

   Answer provided in the Addendum.

2. *Several Machine Development shifts are expected to be conducted for SHIP preparation until LS2. Can you better quantify the overall structure of these MDs and potential impact on the other CERN users?*

   Answer provided in the Addendum.

3. *For the neutrino detector you rely on the availability of the Goliath magnet. Can you clarify its availability and prepare a fallback solution in case this magnet cannot be made available for SHiP?*

   Answer provided in the Addendum.

4. *The SHIP detector has been modified since the LoI, on which the detector infrastructure costing was based. Could you give more details on how the detector infrastructure costing was estimated now, in particular the infrastructure and power converters for the big magnets and the associated electrical infrastructure.*

   Answer provided in the Addendum.

H) Proposal clarification questions

1. *1. In section 4.5.5 it is difficult to visualize the orientation of the WOM option for the readout of the scintillator veto shield. A drawing would help. e.g where are the PMTs located (in z) in Fig. 4.44?*

   The positions of the two WOMs in a particular section or cell are the same along the z direction as can be inferred from the Figs. 4.38 and 4.39 showing the longitudinal cut of the vacuum vessel with several sections (Fig. 4.38) and one section (Fig. 4.39). The distance in the transverse direction within one section can be inferred from Fig. 4.40 showing the transverse cut view of the vacuum vessel. The typical distance in the transversal plane between the two WOMs in one section is 50 cm.

2. *In table 4.8, are the low momentum pions which are mis-IDed (e.g. 4.8% of 1 GeV/c pions) IDed as muons, or just have a poor likelihood value to be pions?*

   Pions are identified as muons if their muon likelihood exceeds a threshold which has been determined to obtain 95% muon identification effiicency.

3. *It would be useful to absolutely normalize Figs. 4.66 and 4.65 so one could compare signal and background.*

   Figures 4.65 and 4.66 are meant to show the interesting momentum range for signal and backgrounds, as the muon identification efficiency and the muon-hadron separation is momentum dependent. However, recent studies on background rejection show that we can reach the goal of < 0.1 background events in five years of data taking using only kinematic and veto requirements. Particle ID detectors will be used to identify the signal final states and to provide additional rejection power that can be used to relax some other cuts. More detailed study will be done for the Technical Design Report.

4. *Section 5.2, p.148: it mentions an assumption of* $4 \cdot 10^6$ *SPS data taking cycles per year, but over 5 years and* $5 \cdot 10^{13}$ *protons/spill, this would lead to* 10^{21} *pot, not* $2 \cdot 10^{20}$*. So presumably the right number is* $1 \cdot 10^6$ *SPS cycles/year?*

   This is correct. Apologies for the typo!

5. *Fig. 5.4 would be useful to see this as a ratio, particularly at low momentum where differences are most significant, given the various detector efficiency dependences on momentum.*

   Figure 12 shows the original Fig. 5.4 of the TP (left) and the ratios of the muon rates for different target configurations (right). The difference of the other configurations with respect to the baseline design with tungsten is $< 20\%$. However it should be noted that the momentum spectrum of muons reaching the sensitive detectors is very different compared to the momentum spectrum shown in this figure.

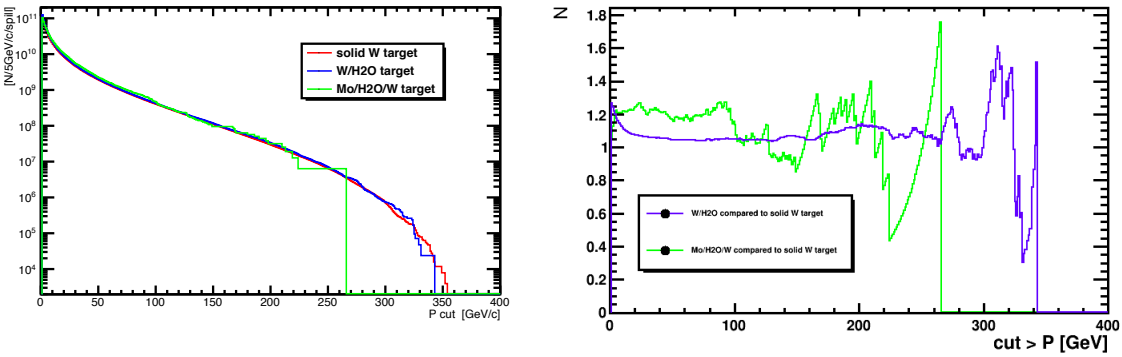

Figure 12: The muon rate after the target and absorber is shown for the different target configurations (left) and as a ratio of different configurations (left). The difference of the other configurations with respect to the baseline design with tungsten is $< 20\%$.

6. *Is it correct in section 5.1.1 that the study validating the muon flux prediction is only in the range* $0.5 < E_\mu < 5$ *GeV? The SHIP muon flux extends to 350 GeV, so the bulk of the energy range is not tested in this validation study, if I read the text above table 5.1 correctly.*

   This is a typo. Thanks for spotting this out. The CHARM data contained no muons with E < 5 GeV.

7. *Are interactions of secondaries in the target included in calculating the signal and background muon and neutrino fluxes?*

   Answer provided in the Addendum.

8. *Does table 5.4 include the contribution from anti-neutrinos?*

   No, it does not. The updated numbers of neutrino and anti-neutrino interactions in the detector material with at least two reconstructed tracks in the detector are shown in the Addendum.

9. *Is there a typo in the text of par. 1 of section 5.2.1.3: with 7 kHz of fully reconstructed beam muons per spill, how can only O(10) enter the decay volume (for use in seeding the toy MC simulation of combinatorial background)?*

   We did not have the CPU power to simulate full spill of 5×10^{13} pot. So, the rate of 7 kHz is an extrapolation based on the simulated statistics ($\sim 10^{11}$ pot), O(10) is the real number of tracks seen in this simulation. The distributions of this tracks have been used as a seed for the toy MC.

10. *In table 5.6: it would be useful to add a column which is the upper limit that can be derived from the MC statistics used to estimate the expected background. For example, the text at bottom p. 162 explains that the upper limit on background from cosmic muons with* $p < 100$ *GeV/c is 12 events, however in the table the expected background is 0 (MC). It would be helpful to summarize this all in the table.*

Answer provided in the Addendum.

11. *Fig.5.18 (p.169), the low impact-parameter-to-target for the $\mu\mu\nu$ channel relative to the neutrino background presumably comes about because the (squared) mass of the HNL (100 MeV) is much lower than the typical Q^2 of the neutrino interactions. Up to what HNL mass can the impact-parameter to target be used effectively to reject neutrino backgrounds?*

    Answer provided in the Addendum.

12. *Fig. 5.18 and Table 5.12(p.171): in the table, $IP < 2.5$ m rejects all 7 MC events, yet from the figure it looks like $\sim$ 50% of the neutrino background would persist with a cut of $IP < 2.5m$.*

    Figure 5.18 of the TP shows the distribution of the IP of neutrino-induced background with the only requirement to have at least two tracks reconstructed in the HS spectrometer. The IP distribution of the neutrino-induced background after all the selection cuts (but the IP one) and the veto requirements is shown in Fig. **??**, left, red curve. We see that 15% of remaining events have an IP$<$ 2.5 m. We have estimated to have $\sim$ 7 events in $N_{\rm pot} = 2 \cdot 10^{20}$, hence $\sim$ 1 event below 2.5 m.

13. *In Section 5.2.2 is the HNL production is estimated using a molybdenum target (as in the text below eqn. 5.2) or the actual tungsten + molybdenum design?*

    The dominant part of the primary proton interactions takes place in the molybdenum target. For the estimate of the signal yield, the molybdenum cross section has been used assuming that all protons interacted there (no charm production in the tungsten part). For actual simulation, charm have been produced in proton-on-proton interactions, then placed inside the target in accordance with the specific interaction lengths.

14. *In Section 5.2.2.2 is the requirement of 25 measurements per track in just the HS spectrometer, or over all of the HS detectors?*

    We required 25 measurements in the HS spectrometer.

15. *It would be useful to see a similar acceptance table in section 5.2.4 for the hidden sector search (or a representative mode) as for the HNL search, to understand what detector performance metrics drive the search sensitivity.*

    Answer provided in the Addendum.

16. *In section 5.2.4, what's the uncertainty on the limits for dark photons for large γ' masses associated with the uncertainty on the calculations of Bremsstrahlung of γ' from partons (given that this is low Q^2 where not only scale uncertainties come in, but also higher-twist corrections)?*

    The calculation of the proton bremsstrahlung contribution to the dark photon production at SHiP is performed in the SHiP Physics Proposal [6]. No estimate of the theoretical uncertainties are presented there, however, the problem is well recognized as indicated in p. 25 of the Physics Proposal: *It is fair to say that at this point there are no universally*

accepted calculational tools available for the computation of production rates and distributions of extra vector states in pp and pn collisions over a wide range of incident energies and for all values of masses mV . We expect that in the future more theoretical work will be done to fill the needs of the SHiP experiment.

The bremsstrahlung contribution to the dark photon production has been calculated for the JPARC and MINOS proton beams (30 GeV and 120 GeV) in Ref. [7]. The theoretical uncertainties have been estimated by varying the normalization scale of PDF from double to half of the dark photon mass: the production cross section changes by less than 30% for the mass of 1 GeV. For the SHiP case this type of uncertainty is not higher. Now any investigation of the higher twist corrections is known in literature.

However it is worth noting that the number of event goes as the fourth power of the photon-paraphoton mixing, so any corrections of order one to the production cross section one may expect imply only 20-30% uncertainty in the SHiP sensitivity to the mixing.

17. *What are the specific selection cuts used to reject backgrounds in the light dark matter sensitivity estimate? Fig. 5.37, the statistics appear insufficient to conclude much about the cut optimization.*

    The selection cuts are $E < 20$ GeV and $0.01 < \theta < 0.02$ rad; most of the signal events are concentrated in this region.

18. *Fig.5.36, should the y-axis units be rad?*

    Typo in the caption: mrad $\rightarrow$ rad.

References

[1] LBNE Collaboration, C. Adams et al., The Long-Baseline Neutrino Experiment: Exploring Fundamental Symmetries of the Universe, arXiv:±1307.7335.

[2] "A facility to Search for Hidden Particles at the CERN SPS: the SHiP physics case" CERN-SPSC-2015-017 ; 8 April 2015.

[3] SHiP collaboration, "A Facility to Search for Hidden Particles (SHiP) at the CERN SPS" CERN-SPSC-2015-016 ; 8 April 2015.

[4] C. Lourenco and H. Wohri, Heavy flavour hadro-production from fixed-target to collider energies, *Phys.Rept.* **433**, 127180, (2006).

[5] R. Ball et al. [NNPDF collaboration], Nucl.Phys. **B809** (2009) 1-63, Nucl. Phys.**B816** (2009) 293.

[6] S. Alekhin et al., "Search for Hidden Particles (SHiP): Physics Proposal" CERN-SPSC-2015-017 ; 9 April 2015, arXiv:1504.04855.

[7] P. deNiverville, D. McKeen, A. Ritz, *Signatures of sub-GeV dark matter beams at neutrino experiments*, arXiv:1205.3499.